

PAPER • OPEN ACCESS

Petrophysical analysis to determine the hydrocarbon prospectivity of sands in AA field, Niger Delta

To cite this article: T. A. Adagunodo and I. A. Akinlabi 2024 *IOP Conf. Ser.: Earth Environ. Sci.* **1342** 012042

View the [article online](#) for updates and enhancements.

You may also like

- [Evaluating Bangestan reservoirs and targeting productive zones in Dezful embayment of Iran](#)
Aynur Nasser, Mohammad Jafar Mohammadzadeh and Seyyed HashemTabatabaee
- [Pore-facies as a tool for incorporation of small-scale dynamic information in integrated reservoir studies](#)
A Chehrizi, R Rezaee and H Rahimpour
- [Estimating petrophysical reservoir properties through extended elastic impedance inversion: applications to off-shore and on-shore reflection seismic data](#)
Mattia Aleardi



PRIME
PACIFIC RIM MEETING
ON ELECTROCHEMICAL
AND SOLID STATE SCIENCE

HONOLULU, HI
October 6-11, 2024

Joint International Meeting of
The Electrochemical Society of Japan (ECSJ)
The Korean Electrochemical Society (KECS)
The Electrochemical Society (ECS)

Early Registration Deadline:
September 3, 2024

**MAKE YOUR PLANS
NOW!**

Petrophysical analysis to determine the hydrocarbon prospectivity of sands in AA field, Niger Delta

T. A. Adagunodo ^a and I. A. Akinlabi ^b

^a Department of Physics, Covenant University, P.M.B. 1023, Ota, Ogun State, Nigeria

^b Department of Earth Sciences, Ladoké Akintola University of Technology, P.M.B. 4000, Ogbomoso, Oyo State, Nigeria

(T. A. Adagunodo Orcid's No: 0000-0001-7810-3323)

*Correspondence: theophilus.adagunodo@covenantuniversity.edu.ng; iaakinlabi@lautech.edu.ng

Abstract. Petrophysical analysis is a crucial process in the oil and gas industry. It entails the analysis and interpretation of well logs, fluid samples or core samples to understand the behaviour of the embedded reservoirs in the subsurface. Three well logs from AA field were provided for this study, but two well data were finally loaded to the workstation due to absence of key well logs (such as gamma ray and density logs) from the third well. The quality control check of the data was done prior to the uploading of data. Delineation of lithologies and identification of hydrocarbon reservoirs were done; the identified reservoirs were correlated across the two wells; and the petrophysical evaluation (such as estimations of shale volume, porosity, permeability and water/hydrocarbon saturation) of the three pay zones (that is, Sand A, B and C) in AA field were done. The porosity of Sands A, B and C varied from 0.27 to 0.28, 0.24 to 0.30 and 0.27. The permeability of Sands A, B and C varied from 1012 to 1314 md, 884 to 1013 md and 692 to 892 md. Meanwhile, the hydrocarbon saturation for Sands A, B and C varied from 1 to 89%, 45 to 80% and 79 to 80%, respectively. It can be concluded that the order of hydrocarbon prospectivity of the reservoir sands correlated across Well AA-1 and Well AA-2 is Sand C > Sand B > Sand A.

Keywords: Geophysics, Hydrocarbon prospectivity, Petrophysics, Reservoir, Well logs

1. Introduction

Petrophysics deals with the study of physicochemical properties of rocks and its interaction with the fluid in the subsurface. Petrophysical analysis of well logs entails transformation of well log measurements into reservoir properties such as lithology, permeability, porosity, fluid content and saturation. A detailed and efficient petrophysical analysis would be able to determine the decisions on exploration, development and production strategies in the oil and gas settings.

Petrophysical analysis of hydrocarbon reservoir sands penetrated in a petroleum field is an integral part of the field's economic assessment exercise. It entails delineation of the geological formation associated with hydrocarbon accumulation in the field, identification of hydrocarbon reservoirs and fluid type, determination of fluid contacts; as well as estimation of effective porosity, water saturation, hydrocarbon saturation, and hydrocarbon volume per unit reservoir volume. The generated information is employed in post-discovery review seismic mapping to locate appraisal wells for ascertaining extent of the penetrated reservoirs and estimating the reserve [1, 2, 3]. The aim of this project is to qualitatively and quantitatively estimate petrophysical parameters in AA field with a view to accurately determine the hydrocarbon in-place. The objectives of this study are to: determine hydrocarbon bearing sands; estimate volume of shale; estimate porosity (total and effective); estimate permeability; and estimate water/hydrocarbon saturation in the study area.



The AA field is an offshore field in the Niger Delta (Fig. 1). The Niger Delta Basin has been described from literature as one of the seven basins in Nigeria [Fig. 1] and most prolific basin in Africa [4, 5]. The petroleum system of the Niger Delta is of the tertiary Akata-Agbada petroleum system. Three major lithostratigraphic sequences present in the Niger Delta are transgressive marine Akata shale, petroliferous paralic Agbada Formation, and the continental Benin sands. Shales are the major cap rocks, which act as seal, while sands and/or sandstones are the reservoirs that entrap the hydrocarbon in the Niger Delta. Details of the petroleum system, sealing nature of the reservoirs and lithostratigraphic units of the Niger Delta have been discussed in articles [4], [5], [6] and [7].

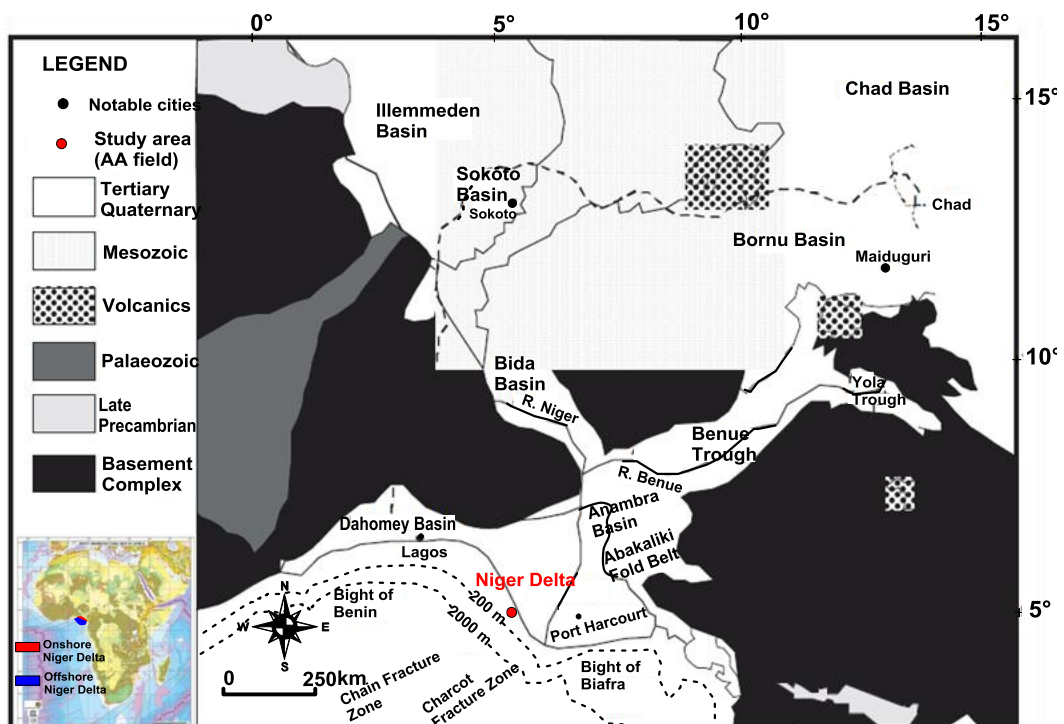


Fig. 1: Geological settings of Nigeria showing the study area

2. Data Availability and Methods

Suites of Six geophysical well logs were imported and used for lithologic identification and to check the quality of the different fluid types and contacts. The logs are gamma ray, caliper, resistivity, sonic, neutron porosity and bulk density logs (Table 1). Out of the three wells for which well logs were provided, two were used for this work due to absence of key well logs like gamma ray and density logs from the third well.

The data sets were sorted into formats, which are compatible with the software used in this study. All data files were stored in a location on the computer, from where they were accessed, prior to their upload to the Geolog software. Fig. 2 shows the workflow of the adopted method in this study.

Table 1: List of available and unavailable well logs and deviation data

Well Name	Gamma Ray (GR)	Caliper (CAL)	Resistivity (RES)	Neutron (NEU)	Density (DEN)	Sonic	Deviation
Well AA-1	✓	✓	✓	✓	✓	✓	x
Well AA-2	✓	✓	✓	✓	✓	✓	x
Well AA-3	x	✓	x	✓	x	✓	x

✓ Available, x Unavailable

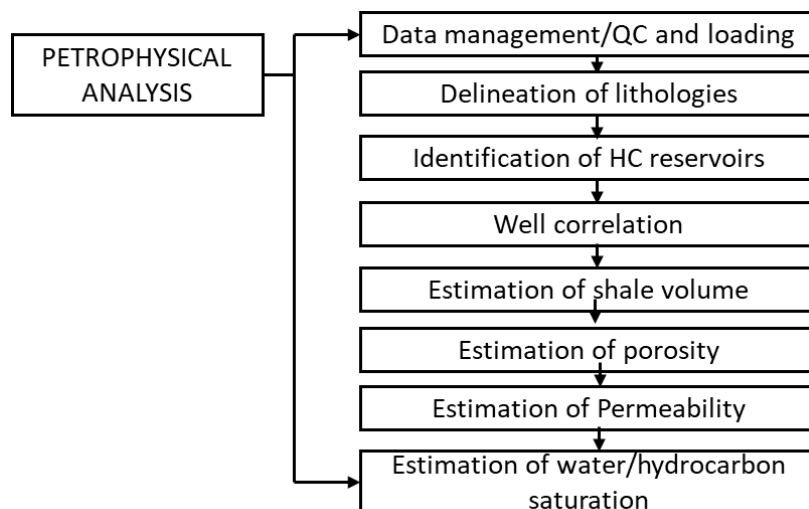


Fig. 2: Project Workflow

2.1 Petrophysical Analysis

Data quality control was carried out before the loading of data so as to ensure needful parameters were given and are arranged accordingly. The sequence of data loading begins with the well header information and logs. The logs (gamma ray, caliper, resistivity, density, sonic and neutron) were then imported for wells AA-1 and AA-2, respectively. Rescaling of each of the logs was carried out and necessary adjustment was applied to logs where applicable, this was to enhance visual logs interpretation. The petrophysical parameters in this study were determined from the applications of Eq. (1) to Eq. (10) to the data obtained for this study.

2.1.1 Volume of Shale (V_{sh})

Shale volumes were evaluated using Gamma ray (GR) method. GR logs were used in the evaluation because the adopted wells have GR logs; Larionov method was chosen because it goes well with Tertiary Niger delta rocks and is widely used in the industry [5, 8, 9].

The picking of parameters that will be needed for the estimation of the volume of shale was done via the frequency plot of the gamma ray to show the distribution of shale and sand within the reservoir. The GR index was calculated using Eq. (1), which was adopted from the Larionov formulae.

$$I_{GR} \equiv \frac{GR - GR_{\min}}{GR_{\max} - GR_{\min}} \quad (1)$$

where GR is the gamma ray log reading in the zone of interest, GR_{\min} is the minimum GR log reading zone of interest and GR_{\max} is the maximum GR log reading in the zone of interest. For tertiary rocks (such as Niger Delta), the volume of shale is estimated using Eq. (2).

$$V_{sh} \equiv 0.083 \times (2^{(3.7 \times I_{GR})} - 1) \quad (2)$$

2.1.2 Porosity (ϕ)

Porosity is defined as the percentage of voids to the total volume of rock. Porosity parameters were picked with the choice of cross plotting density and neutron logs. The choice of density-neutron log for picking porosity values was dependent on the fact that the logs are available. Total porosity was estimated majorly from density logs using a rho-matrix value of 2.65 gm/cc and rho-fluid value of 0.808 gm/cc from pressure, volume and temperature data. The effective porosity was then deduced by introducing shale volume into the equation.

All porosity was computed from the parameter picked, using the Bateman and Konen method of porosity calculation as shown in Eq. (3), which was given by [10].

$$\phi \equiv \left[\frac{\phi^2_N + \phi^2_D}{2} \right]^{1/2} \quad (3)$$

This include calculation of total porosity and porosity of interconnected pore space (effective porosity), that will be computed in the report. Eq. (4) to Eq. (6) were used in the computation.

$$\phi_T \equiv \frac{\rho_{ma} - \rho_B}{\rho_{ma} - \rho_f} \quad (4)$$

$$\phi_{Tsh} \equiv \frac{\rho_{ma} - \rho_{sh}}{\rho_{ma} - \rho_f} \quad (5)$$

$$\phi_E \equiv \phi_T - (\phi_{Tsh} \times V_{sh}) \quad (6)$$

where ρ_{ma} is the matrix bulk density, ρ_{sh} is the shale bulk density, ρ_f is the fluid density (density log reading in 100% water), ρ_B is the bulk density (density log reading in the zone of interest), V_{sh} is the volume of shale, ϕ_T is the total porosity in the zone of interest, ϕ_{Tsh} is the total porosity in shale and ϕ_E is the effective porosity in the zone of interest.

2.1.3 Water Saturation

Water saturation was estimated from Simandoux equations since the reservoirs of interest are not “clean”. In order to estimate water saturation from any of the methods, formation water resistivity (R_w) was first calculated.

However, deep resistivity (R_t) and ϕ (porosity) may vary widely within the water-bearing zone making it difficult to get single values for each of them. For this reason, a double logarithmic plot of deep resistivity against porosity is generally used to estimate formation water resistivity. Formation water resistivity is the intersection on the deep resistivity axis of a best fit line produced from the plot. The plot is commonly referred to as “Picket plot”.

In this study, a Picket plot was used in estimation of formation water resistivity from water-bearing interval. Therefore, the water saturation was then estimated using the computed formation water resistivity and porosity; local correction factor or tortuosity factor (a) of 1 was assumed; saturation exponent (n) of 2 was also assumed; and cementation exponent (m) of 1.80 to 1.82 were used in this study [5, 8]. Effective porosity saturation was estimated using Simandoux equation by taking cognisance of volume of shale (V_{sh}) as shown in Eq. (7) and Eq. (8).

$$\frac{1}{R_t} \equiv \frac{S_w^2}{F \times R_w (1 - V_{sh})} + \frac{V_{sh} \times S_w}{R_{sh}} \quad (7)$$

$$BVWE = S_{we} * \phi_e \quad (8)$$

Note that R_w is the formation water resistivity, R_t is the formation resistivity, ϕ_e is the calculated porosity, V_{sh} is the calculated volume of shale in the zone of interest, R_{sh} is the resistivity of log reading in 100% shale, $BVWE$ is the effective bulk volume of water, F is the formation resistivity factor and S_h is the hydrocarbon saturation.

2.1.4 Permeability (K)

The permeability was calculated using the Tixier permeability expression [11]. This was achieved by using the calculated effective porosity log as shown in Eq. (9).

$$K \equiv \left(250 * \frac{\phi_{eff}^3}{S_{wlrr}} \right)^2 \quad (9)$$

where K is the permeability, Φ_{eff} in the effective porosity and S_{wlrr} is the irreducible water saturation.

2.1.5 Hydrocarbon Saturation (S_h)

The hydrocarbon saturation which is the percentage of pore volume in a formation occupied by hydrocarbons was obtained by using Eq. (10).

$$S_h \equiv (100 - S_w)\% \quad (10)$$

where S_h is the hydrocarbon saturation and S_w is the water saturation.

3. Results and Discussion

3.1 Interpretation of Sand A Features

In Well AA-1, Sand A is a wet sand with a measure depth of about 6023 ft (1835.81 m) and 6182 ft (1884.274 m) at the top and base, respectively. The reservoir gross interval thickness is 158ft (48.1584 m), net-pay thickness 141 ft (42.9768 m) and the net-to-gross (N/G) ratio is 0.89. The porosity is 27%, effective porosity is 26%, water saturation is 99%, hydrocarbon saturation 1%, permeability is 1058 md and the volume of shale is 8%. From the calculated parameters (Table 2), the reservoir has a good pay thickness with high net-to-gross, low volume of shale, good porosity value, good permeability, but very poor hydrocarbon saturation; hence, Sand A is a wet reservoir (Fig. 3).

In Well AA-2 as shown in Fig. 4, most of the sands present appear to be of low resistivity pay zones. The highest resistivity value obtained is 13 ohm.m, while the lowest value is between 1 – 4 ohm.m. Sand-A has a reservoir gross interval thickness of 111 ft (33.8328 m), net-pay thickness of 87 ft (26.5176 m) and a net-to-gross (N/G) ratio of 0.79. The porosity is 28%, effective porosity is 23%, water saturation is 19%, hydrocarbon saturation is 89%, permeability is 1012 md and the volume of shale is 8.5%. From the calculated parameters (Table 2), the reservoir has good pay thickness with good net-to-gross, low volume of shale, good porosity value, good permeability and very good hydrocarbon saturation; hence, Sand A is a good hydrocarbon reservoir. The relative amplitudes of petrophysical parameters of Sand A across the two wells are shown in Fig. 5 and Fig. 6.

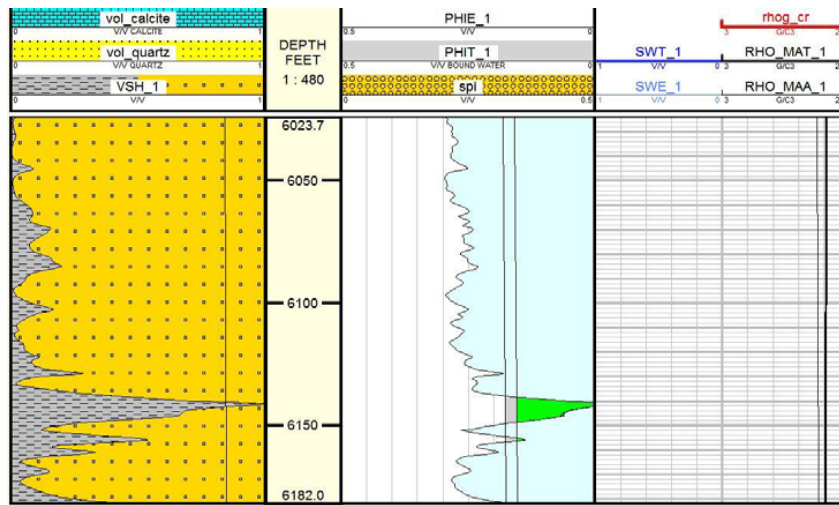


Fig. 3: Calculated petrophysical parameters for Sand A in Well AA-1.

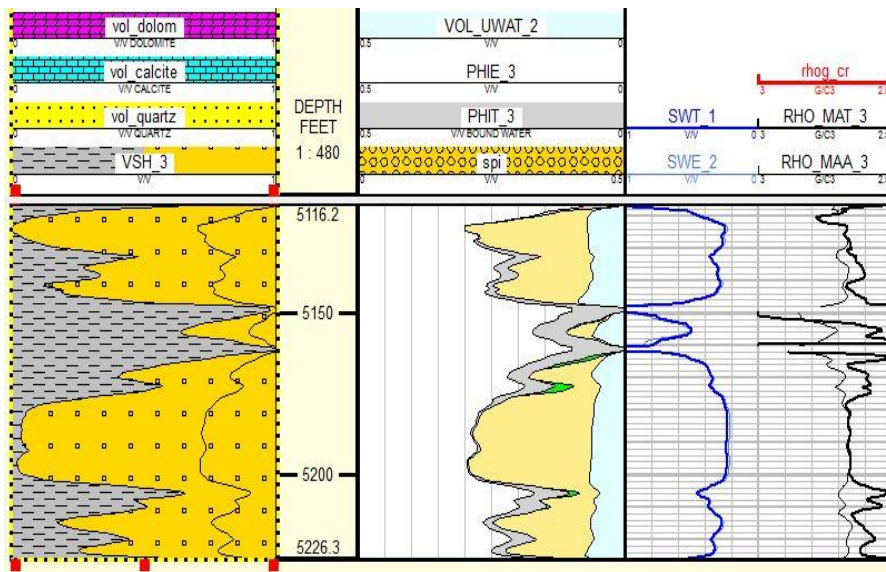


Fig. 4: Calculated petrophysical parameters for Sand A in Well AA-2.

Table 2: Summary of the average computed petrophysical parameters obtained for Sand A

Well	Gross Sand (ft)	Net Sand (ft)	Net/Gross	Shale Volume (%)	Porosity (%)	Effective Porosity (%)	Permeability (md)	Hydrocarbon Saturation (%)	Water Saturation (%)
Well AA-1	158	141	0.89	0.08	0.27	0.26	1058	0.01	0.99
Well AA-2	111	87	0.79	0.085	0.28	0.23	1012	0.89	0.19

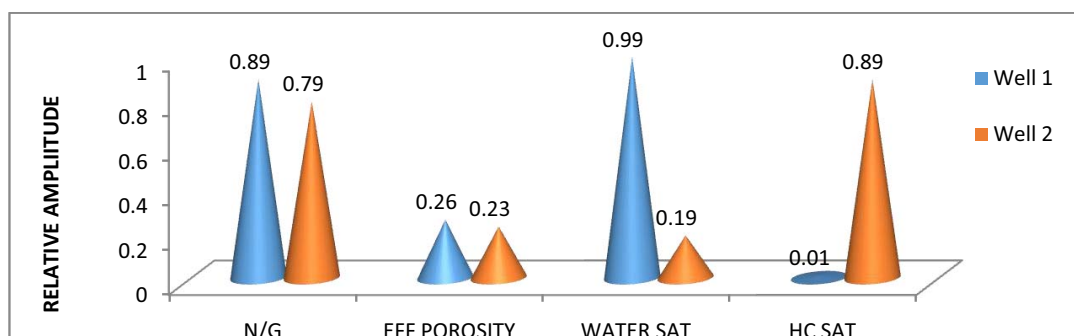


Fig. 5: Ranking of Sand A across the two Wells using average petrophysical parameters.

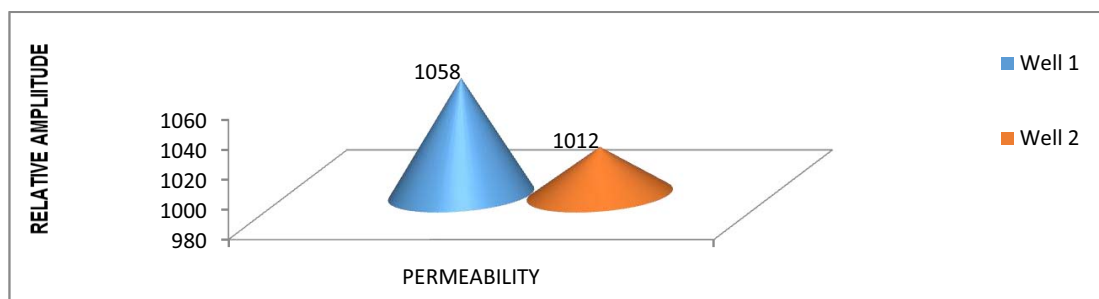


Fig. 6: Ranking of Sand A across the two Wells using average permeability.

3.2 Interpretation of Sand B Features

In Well AA-1, Sand-B is oil bearing sand with an oil-water-contact (OWC) of about 6667.00 ft (2032.102 m) with a measured depth of about 6607 ft (2013.814 m) and 6798 ft (2072.03 m) at the top and base, respectively. The reservoir gross interval thickness is 191 ft (58.2168 m), net-pay thickness is 160 ft (48.768 m) and the net-to-gross (N/G) ratio is 0.84. The porosity is 24%, with effective porosity of 15%, water saturation of 55%, hydrocarbon saturation of 45%, permeability of 884 md and the volume of shale is 4%. From the calculated parameters

(Table 3), the reservoir of Sand B has good pay thickness with good net-to-gross, low volume of shale, good porosity value, intermediate permeability and low hydrocarbon saturation; hence, Sand B is a poor hydrocarbon reservoir (Fig. 7).

In Well AA-2, Sand-B has reservoir gross interval thickness of 174 ft (53.0352 m), net-pay thickness of 124 ft (37.7952 m) and net-to-gross (N/G) ratio of 0.71. The porosity is 30%, effective porosity is 19%, water saturation is 20%, hydrocarbon saturation 80%, permeability is 1013 md and the volume of shale is 5%. From the calculated parameters (Table 3), the reservoir has a good pay thickness with a good net-to-gross, low volume of shale, good porosity value, good permeability and good hydrocarbon saturation; hence, Sand B is a good hydrocarbon reservoir (Fig. 8). The relative amplitudes of petrophysical parameters of Sand B across the two wells are shown in Fig. 9 and Fig. 10.

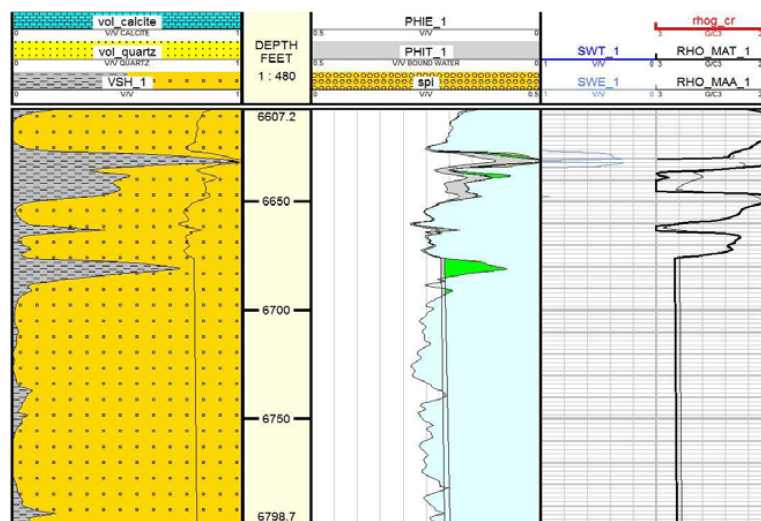


Fig. 7: Calculated petrophysical parameters for Sand B in Well AA-1.

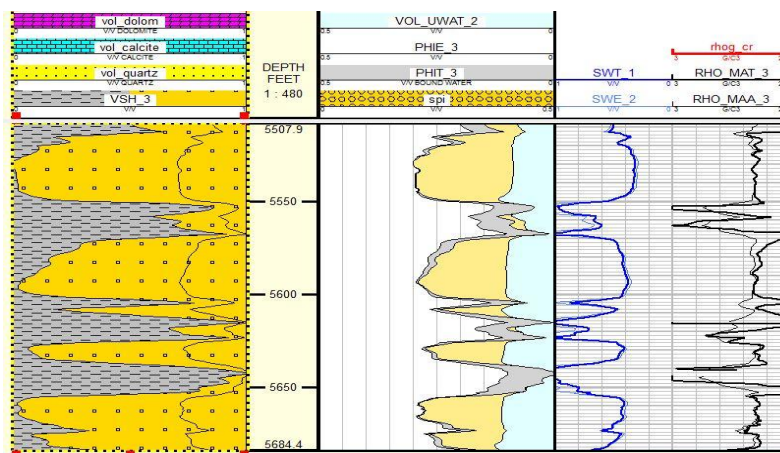


Fig. 8: Calculated petrophysical parameters for Sand B in Well AA-2.

Table 3: Summary of the average computed petrophysical parameters obtained for Sand B

Well	Gross Sand (ft)	Net Sand (ft)	Net/Gross	Shale Volume (%)	Porosity (%)	Effective Porosity (%)	Permeability (md)	Hydrocarbon Saturation (%)	Water Saturation (%)
Well AA-1	191	160	0.84	0.04	0.24	0.15	884	0.45	0.55
Well AA-2	174	124	0.71	0.05	0.30	0.19	1013	0.80	0.20

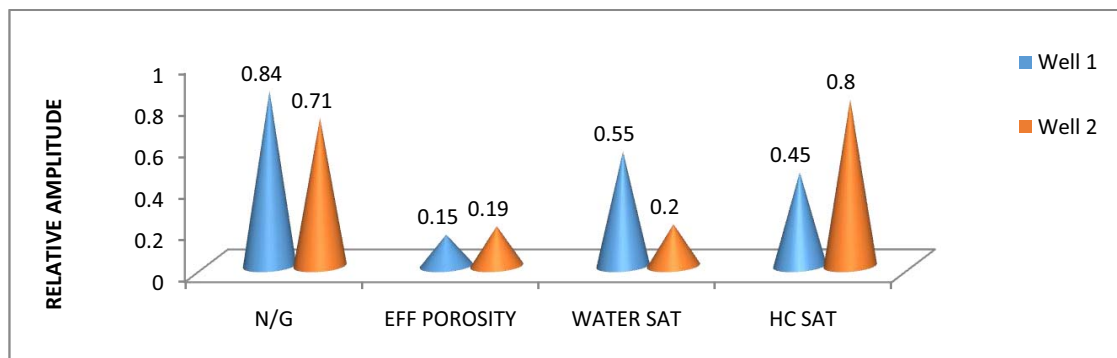


Fig. 9: Ranking of Sand B across the two wells using average petrophysical parameters.

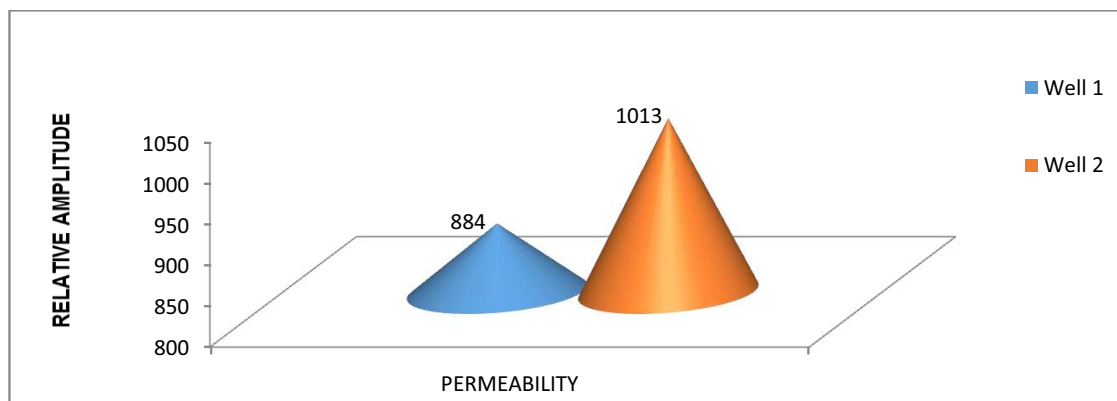


Fig. 10: Ranking of Sand B across the two wells using average permeability.

3.3 Interpretation of Sand C Features

In Well AA-1, Sand-C has reservoir gross interval thickness of 127 ft (38.7096 m), net-pay thickness 119 ft (36.2712 m) and a net-to-gross (N/G) ratio of 0.93. The porosity is 27%, effective porosity is 22%, water saturation is 20%, hydrocarbon saturation 80%, permeability is 892 md and the volume of shale is 3%. From the calculated parameters (Table 4), the reservoir has a high pay thickness with high net-to-gross, low volume of shale, good porosity value, intermediate permeability and very good hydrocarbon saturation; hence, Sand C is a good hydrocarbon reservoir (Fig. 11).

In Well AA-2, Sand-C has a reservoir gross interval thickness of 187 ft (56.9976 m), a net-pay thickness of 117 ft (35.6616 m) and a net-to-gross (N/G) ratio of 0.62. The porosity is 27%, effective porosity is 23%, water saturation is 21%, hydrocarbon saturation 79%, permeability is 692 md and the volume of shale is 11%. From the calculated parameters (Table 4), the reservoir has a good pay thickness with a good net-to-gross, a low volume of shale, a good porosity value, an intermediate permeability and good hydrocarbon saturation; hence, Sand C is a good hydrocarbon reservoir (Fig. 12). The relative amplitudes of petrophysical parameters of Sand C across the two wells are shown in Fig. 13 and Fig. 14.

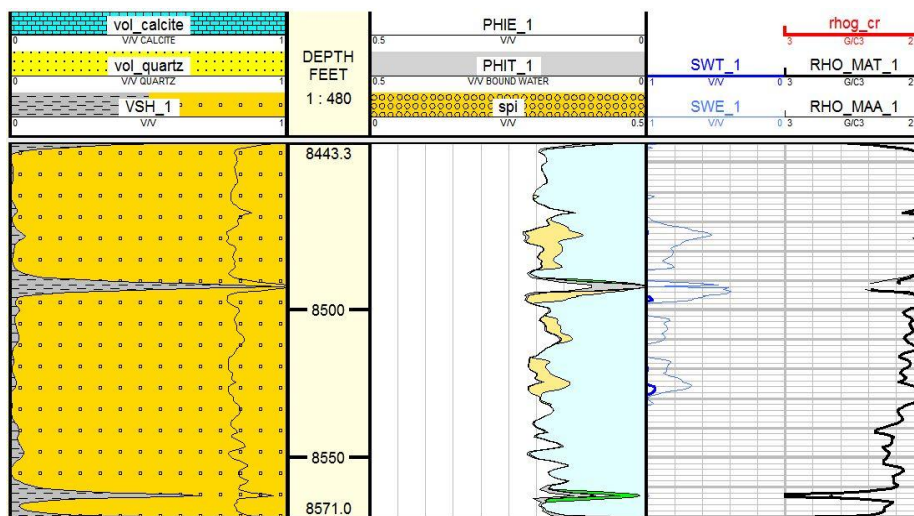


Fig. 11: Calculated petrophysical parameters for Sand C in Well AA-1.

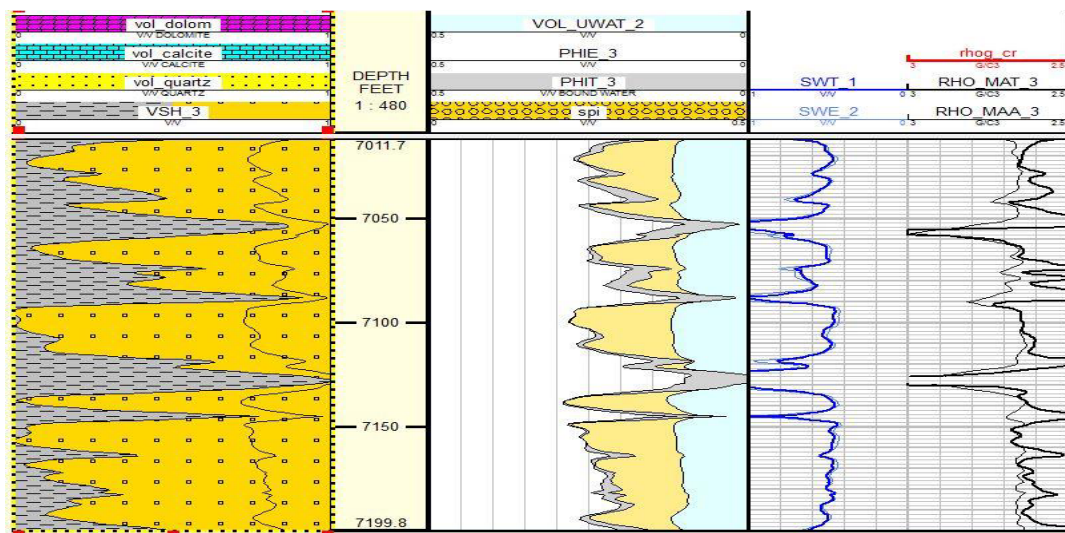


Fig. 12: Calculated petrophysical parameters for Sand C in Well AA-2.

Table 4: Summary of the average computed petrophysical parameters obtained for Sand C

Well	Gross Sand (ft)	Net Sand (ft)	Net/Gross	Shale Volume (%)	Porosity (%)	Effective Porosity (%)	Permeability (md)	Hydrocarbon Saturation (%)	Water Saturation (%)
Well AA-1	127	119	0.93	0.03	0.27	0.22	892	0.80	0.20
Well AA-2	187	117	0.62	0.11	0.27	0.23	692	0.79	0.21

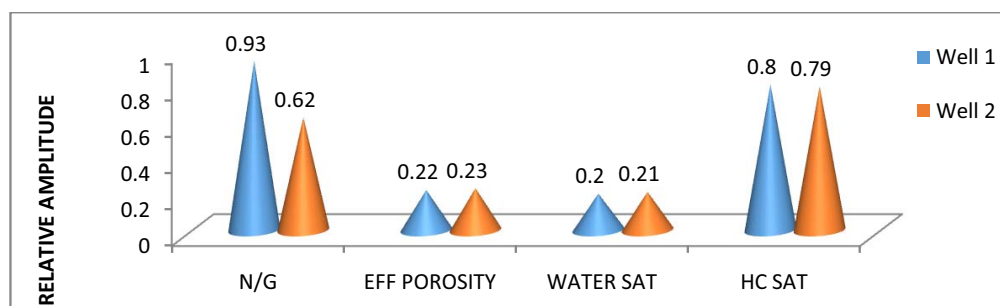


Fig. 13: Ranking of Sand C across the two Wells using average petrophysical parameters.

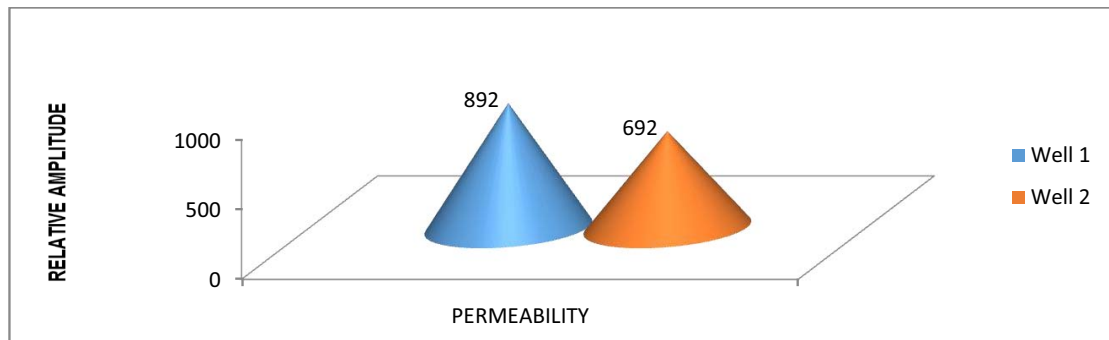


Fig. 14: Ranking of Sand A across the two Wells using average permeability.

4. Conclusion and Recommendation

Petrophysical evaluation of the reservoirs revealed that the quality of porosity and permeability of the pay zones varied from intermediate to very good. There was a gradual decrease in porosity and permeability values with depth, most likely, as a result of compaction associated with depth of burial of the older sediments as deposition occurred. A decrease in water saturation is observed as the hydrocarbon saturation increases across the reservoir sands. Further, an increase in the net-to-gross value was noticed when the hydrocarbon saturation increases. The analyses revealed that: Sand A reservoir in Well AA-1 is wet, while that of Well AA-2 contains hydrocarbon; Sand B reservoir in Well AA-1 and Well AA-2 contained fair to good percentage of hydrocarbon; and Sand C reservoir in Well AA-1 and Well AA-2 contained an appreciable volume of hydrocarbon. It can be concluded that the order of hydrocarbon prospectivity of the reservoir sands correlated across Well AA-1 and Well AA-2 is Sand C > Sand B > Sand A. This indicates that Sand C is the most productive reservoir, while Sand A is the least productive reservoir in AA field. With reference to the petrophysical analysis carried in this study, the following are recommended:

- i. seismic interpretation should be carried out so as to delineate the Gross Rock Volume of the reservoirs which is an input in estimating the oil initially in place (or OOIP);
- ii. conventional core should be taken within the reservoir interval to properly characterize the reservoir and reduce uncertainties; and
- iii. complete logging while drilling (LWD) suites should be conducted when drilling the next well in AA field.

Acknowledgement

We appreciate the contributions from the ICSSD 2023 Editorial Board and the reviewers for improving the quality of this paper. The support received from Covenant University is highly appreciated.

Reference

- [1]. Hussain W., Ali N., Sadaf R., Hu C., Nykilla E.E., Ullah A., Iqbal S.M., Hussain A., Hussain S., Petrophysical analysis and hydrocarbon potential of the lower Cretaceous Yageliemu Formation in Yakela gas condensate field, Kuqa depression of Tarim Basin, China. *Geosystems and Geoenvironment*, 2022, 1, 100106. <https://doi.org/10.1016/j.geogeo.2022.100106>.
- [2]. Senosy A.H., Ewida H.F., Soliman H.A., Ebraheem M.O., Petrophysical analysis of well logs data for identification and characterization of the main reservoir of Al Baraka oil field, Komombo Basin, Upper Egypt. *SN Applied Sciences*, 2020, 2, 1293. <https://doi.org/10.1007/s42452-020-3100-x>.
- [3]. Sudi A.H.P., Sitaresmi R., Yulia P.S., Petrophysical analysis to determine the initial oil reserves in the AHP field. *IOP Conf. Series: Earth and Environmental Science*, 2021, 819, 012021. <https://doi.org/10.1088/1755-1315/819/1/012021>.
- [4]. Bayowa O.G., Adagunodo T.A., Oshonaiye A.O., Boluwade B.S., Mapping of thin sandstone reservoirs in Bisol field, Niger Delta, Nigeria using Spectral Decomposition (SD) technique. *Geodesy and Geodynamics*, 2021 12(1), 54 – 64. <https://doi.org/10.1016/j.geog.2020.11.002>.
- [5]. Adagunodo T.A., Sunmonu L.A. and Adabanija M.A., Reservoir Characterization and Seal Integrity of Jemir Field in Niger Delta, Nigeria. *Journal of African Earth Sciences*, 2017, 129, 779 – 791. <https://doi.org/10.1016/j.jafrearsci.2017.02.015>.
- [6]. Oyeyemi K.D., Olowokere M.T., Aizebeokhai A.P., Hydrocarbon resource evaluation using combined petrophysical analysis and seismically derived reservoir characterization, offshore Niger Delta. *Journal of Petroleum Exploration and Production Technology*, 2018, 8, 99 – 115. <https://doi.org/10.1007/s13202-017-0391-6>.
- [7]. Oyeyemi K.D., Olowokere M.T., Aizebeokhai A.P., Building 3D lithofacies and depositional models using sequential indicator simulation (SISIM) method: a case history in western Niger Delta. *Arabian Journal for Science and Engineering*, 2018, 43, 3775 – 3792. <https://doi.org/10.1007/s13369-018-3212-4>.
- [8]. Adagunodo T.A., Bayowa O.G., Alatis O.E., Oshonaiye A.O., Adewoyin O.O., Opadele V.O., Characterization of reservoirs and depositional study of J-P field, shallow offshore of Niger Delta Basin, Nigeria. *Scientific African*, 2022, 15, e01064. <https://doi.org/10.1016/j.sciaf.2021.e01064>.
- [9]. Bayowa O.G., Adagunodo T.A., Oyedara I.I., Reservoir Classification and Petrophysical Evaluation of “BAO” Field, Niger Delta. *Petroleum and Coal*, 2019, 61(5), 1112 – 1119. https://www.vurup.sk/wp-content/uploads/2019/09/PC-X-2019_Adagunodo_98.pdf.
- [10]. Bateman R.M. and Konen C.E., The log analyst and the programmable pocket calculator. *Log Analyst*, September – October 1977, 18(5), 3 – 10.
- [11]. Tixier M.P., Evaluation of permeability from electrical-log resistivity gradients. *Oil and Gas Journal*, June 1949, 113.